*International Journal of Applied Glass Science 3 [4] 369–379 (2012)*
*DOI:10.1111/ijag.12004*

INTERNATIONAL JOURNAL OF
Applied Glass
SCIENCE

# Physical and Mechanical Properties of Barium Alkali Silicate Glasses for SOFC Sealing Applications

**Rosa Trejo, Edgar Lara-Curzio,*,† Amit Shyam,* Melanie J. Kirkham, Valerie Garcia-Negron, and Yanli Wang**

*Materials Science & Technology Division, Oak Ridge National Laboratory, Oak Ridge, Tennessee 37831-6062*

The physical and mechanical properties of two barium alkali silicate glasses were determined as a function of temperature. Their Young's modulus and Poisson's ratio were determined by resonant ultrasound spectroscopy; their viscosity, thermal expansion, and glass transition temperature were determined using a thermomechanical analyzer. The wetting behavior of the two glasses on alumina and 8 mol% yttria stabilized zirconia (8YSZ) substrates was determined by measuring contact angles in air as a function of temperature and time. Values of Young's modulus for both glasses were in good agreement with those predicted by the Makishima and MacKenzie model. The physical and mechanical properties of these glasses are discussed in the context of their potential use for sealing applications in solid-oxide fuel cells.

## Introduction

The primary function of seals in planar solid oxide fuel cells (SOFCs) is to prevent mixing of fuel and oxidizing gases during SOFC operation. Seal materials need to be electrically insulating, thermo-chemically stable under both fuel and oxidizing environments and need to exhibit thermal expansion behavior that is compatible with other components of the stack.[1] Seals are also expected to exhibit durability on a time scale comparable to the expected service life of SOFCs, that is, up to 40,000 h.

Crystallization-resistant glasses are leading candidates for SOFC sealing applications because of their self-healing characteristics and ability to relax thermal stresses *via* viscous flow at SOFC operating temperatures.[2–5] Furthermore, these glass systems are attractive because their chemical composition and therefore their viscosity, wetting behavior, thermal expansion, and elastic properties can be tailored to match specific SOFC design requirements.

In this study, we report values of the physical and mechanical properties of two commercially available barium alkali silicate glasses: SCN-1 (SEM-COM Company,



*Member, The American Ceramic Society.
†laracurzioe@ornl.gov

Inc., Toledo, OH) and G6 (Whatman Inc., Piscataway, NJ). Their chemical composition was determined by inductively coupled plasma mass spectroscopy and inductively coupled plasma atomic emission spectroscopy; their Young's modulus and Poisson's ratio were determined as a function of temperature by resonant ultrasound spectroscopy; viscosity, thermal expansion, and glass transition temperature were determined using a thermomechanical analyzer. Their wetting behavior on alumina and 8YSZ substrates was determined by measuring contact angles in air as a function of temperature and time. These properties are necessary to assess the viability of glasses for SOFC sealing applications and the feasibility of incorporating them into specific SOFC designs.

## Experimental Procedure

Two barium alkali silicate glasses were investigated in this study: SCN-1 was obtained in powder form with an average particle size of 10 μm, while G6 was obtained in the form of mats (200-μm thick) that are composed of glass fibers in an organic binder.

Test specimens of SCN-1 glass were prepared by cold-pressing glass powders into cylindrical (9.5 mm diameter and 25 mm in length) or rectangular (25 mm × 37.5 mm × 25 mm) pellets using stainless steel dies. The compressed SCN-1 pellets were subsequently sintered onto 300-μm-thick 8YSZ substrates at 850°C for 2 h in air with heating and cooling rates of 3°C/min. Test specimens of G6 glass were obtained by sintering for two hours at 850°C a stack of disks that had been punched out from the mat and placed onto 300-μm-thick 8YSZ substrates. The desired specimen configurations for the various tests performed in this study were obtained by machining specimens from the sintered pieces using a diamond wheel in diluted (1:15) CIMTECH® 500 Metal working fluid concentrate.

### *Density*

The density of the as-sintered glasses was measured via the Archimedes method using 3 mm × 3 mm × 5mm test specimens. To determine porosity, the cross-section of a sintered glass pellet was prepared metallographically, and images obtained at a magnification of 250× using a scanning electron microscope were analyzed with an image analysis software package (ImageJ; National Institutes for Health, Bethesda, MD).

### *Chemical Composition and Phase ID*

The chemical composition of SCN-1 and G6 glasses was determined by inductively coupled plasma mass spectrometry (ICPMS) and inductively coupled plasma-Atomic Emission Spectrometry (ICPAES). Chemical analysis by ICPMS was performed using an X-Series2 ICP-MS (Thermo Scientific, West Palm Beach, FL) instrument. Data were acquired in peak jump mode and collected with computer-controlled PlasmaLab® software. The ICP-AES used in this study was an IRIS IntrepidII XSP instrument5 with Duoview radial torch. Details about ICPMS and ICPAES analyses can be found elsewhere.[6]

Powders of as-received and sintered SCN-1 glass and fibrous mats of G6 were obtained after crushing them with an agate mortar and pestle. The phase analysis of the powders was performed at ambient conditions by X-ray diffraction (Philips X'PERT PRO MPD X-Ray Diffractometer, Westborough, MA) using Cu $K_\alpha$ radiation at 45 kV and 40 mA over a $2\theta$ range between 8 and 85°. The data were analyzed using a commercial software package (Jade Software; Materials Data Inc., Livermore, CA).

### *Thermal Expansion Behavior and Glass Transition Temperature*

Thermal expansion behavior was determined using a thermomechanical analyzer (TMA) (TMA Q400; TA Instruments, New Castle, DE). Test specimens were heated and cooled at a constant rate of 5°C/min between 25 and 600°C. Test specimens consisted of rectangular parallelepipeds with nominal dimensions of 3 mm × 3 mm × 5 mm. The ends of the test specimen were machined to achieve flatness and parallelism within 0.005 mm. A constant compressive load was maintained over the specimen during the test, and experiments were performed under loads of 0.1, 0.05, and 0.01 N at each cycle to investigate the effect of compressive load on the glass transition temperature.

### *Viscosity*

To determine the viscosity of the glasses, cylindrical test specimens (7.3 mm in diameter and 5.5 mm in height) were core-drilled from blocks of sintered glass using a 100 grit diamond-impregnated steel core drill at 800 rpm. The ends of the cylinder were machined

to ensure flatness and parallelism within 0.005 mm. Measurements were obtained using a TMA[7] that had a 20-mm diameter silica stage and a 3-mm diameter silica probe (TMA Q400; TA Instruments). The cylindrical test specimen was sandwiched between two 0.025-mm-thick platinum foil discs and 0.46-mm-thick quartz discs (Fig. 1). Two different procedures were followed to determine viscosity: (i) isothermal dimensional measurements under a constant compressive mechanical load and (ii) dimensional measurements while heating the specimen at a constant heating rate and a constant compressive mechanical load. For the isothermal tests, the test specimens were heated at 5°C/min and then maintained at 550, 600, 650, 700, and 750°C. At each temperature, the test specimen was held under a constant compressive mechanical load. Tests were performed at load levels of 0.1, 0.25, and 0.5 N at each temperature. The duration of each isothermal segment was 60 min for tests at 550°C, 20 min for tests at 600°C and 650°C, 10 min for 700°C, and 5 min for 750°C. The duration of each segment was selected to ensure a constant viscosity value was attained.

For measurements under a constant heating rate, tests specimens were maintained under a constant compressive load of 0.1 N and heated from 25°C up to 750°C at a constant rate. Tests were performed at heating rates of 1, 5, and 10°C/min.

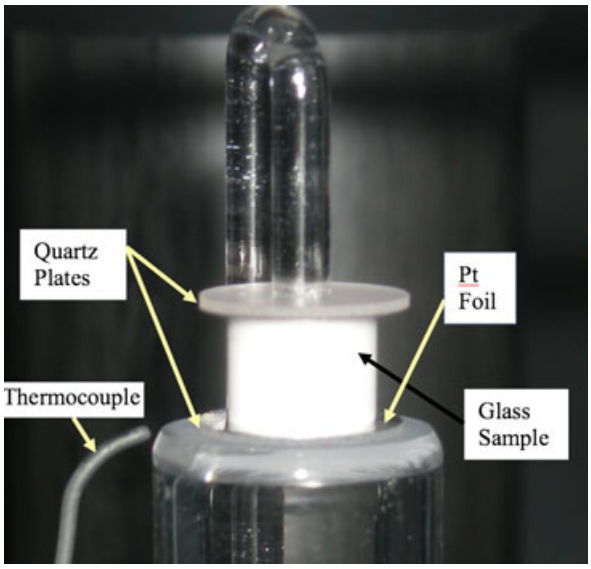


*Fig. 1. Experimental set-up used to determine viscosity using a thermomechanical analyzer (TMA). The test specimen, quartz plates, platinum foil and TMA probe are visible in the picture.*

### *Elastic Constants*

The elastic constants of SCN-1 and G6 were determined up to 600°C by Resonant Ultrasound Spectroscopy (RUS) (Magnaflux Quasar, Albuquerque, NM). Rectangular parallelepiped-shaped specimens were supported by three piezoelectric transducers with one transducer (transmitting transducer) used to generate an elastic wave of constant amplitude and varying frequency, whereas the other two transducers were used to detect the resonance frequencies.[8,9] To obtain resonant spectra at elevated temperatures, test specimens were placed on top of silicon carbide rods, which serve as an extension of the piezoelectric transducers and allow the placement of the test specimen in the hot zone of a cylindrical furnace. A RUS spectrum was acquired and analyzed every 50°C during heating and cooling in ambient air. The spectrum of resonant frequencies obtained cannot be deconvoluted directly to determine the elastic constants. Instead, a spectrum is calculated from the known dimensions of the test specimen, its density and a set of "guessed" elastic constants, and a multidimensional algorithm is used to minimize the root mean square (RMS) error between the measured and calculated resonant peaks. The temperature-dependent specimen dimensions were used in the data analysis. This process was repeated iteratively until the solution converges, and the final spectrum fit enables the estimation of the elastic constants of the solid from a single frequency scan (Galaxy analysis software; Magnaflux Quasar, Albuquerque, NM).

### *Wetting Behavior*

The wetting behavior of SCN-1 and G6 glasses on 8YSZ and $Al_2O_3$ substrates was determined in air as a function of time and temperature. The experimental set-up consisted of a horizontal tubular furnace with a digital camera mounted close to its open end. Compressed powders of SCN-1 or a stack of layers of G6 were placed on top of 300-μm-thick plates of 8YSZ or $Al_2O_3$. Test specimens were heated up at a constant heating rate of 5°C/min to the test temperature and then the temperature was maintained constant for 168 h. Experiments were performed at temperatures between 600 and 900°C. Digital images of the test

specimen were obtained at regular time intervals and were subsequently analyzed using an image analysis program (Contact angle plugin for the ImageJ computer program; National Institute of Health). The surface roughness of the 8YSZ and $Al_2O_3$ substrates varied between 0.40 and 0.55 μm.

## Results

### *Density and Porosity*

The density of as-sintered G6 and SCN-1 glasses was found to be 2.49 and 2.22 g/cm$^3$, respectively. The average porosity of as-sintered SCN-1 test specimens was 18%, while the pore size ranges between 4 and 85 μm in diameter with a mean value of 10 μm. The average porosity in G6 glass was 3%. Figure 2 shows scanning electron micrographs illustrating the microstructure of both glasses in the as-sintered condition.

### *Chemical Composition and Phase ID*

Table I lists the chemical composition in weight% of SCN-1 and G6 glasses determined by ICP-MS and ICP-AES. The precision of chemical composition measurements using ICP-MS and ICP-AES was found to vary depending on individual elements, but in general, ICP-AES was found to have greater precision than ICP-MS.[6] X-ray diffraction analysis showed that after sintering both glasses remained completely amorphous.

### *Thermal Expansion Behavior and Glass Transition Temperature*

The results of three successive thermal expansion measurements on SCN-1 glass carried out under compressive loads of 0.10, 0.05, and 0.01 N are presented in Fig. 3. These load levels correspond to stresses of 11.1, 5.5 and 1.1 kPa. The coefficient of thermal expansion of SCN-1 exhibits a slight temperature dependence that can be expressed as follows between 5 and 400°C.

$$\alpha(T) = 9.97 \times 10^{-6} + (7.79 \times 10^{-9})T \quad (^{\circ}C^{-1}) \quad (1)$$

where $T$ is in degrees Celsius. During heating at about 550°C, the test specimen started to lose rigidity and began to shrink axially as a result of lateral viscous flow. The amount and rate of axial shrinkage, due to lateral glass flow, increased with increasing compressive load. The width of the hysteresis loop therefore, increased with the magnitude of the applied compressive load.

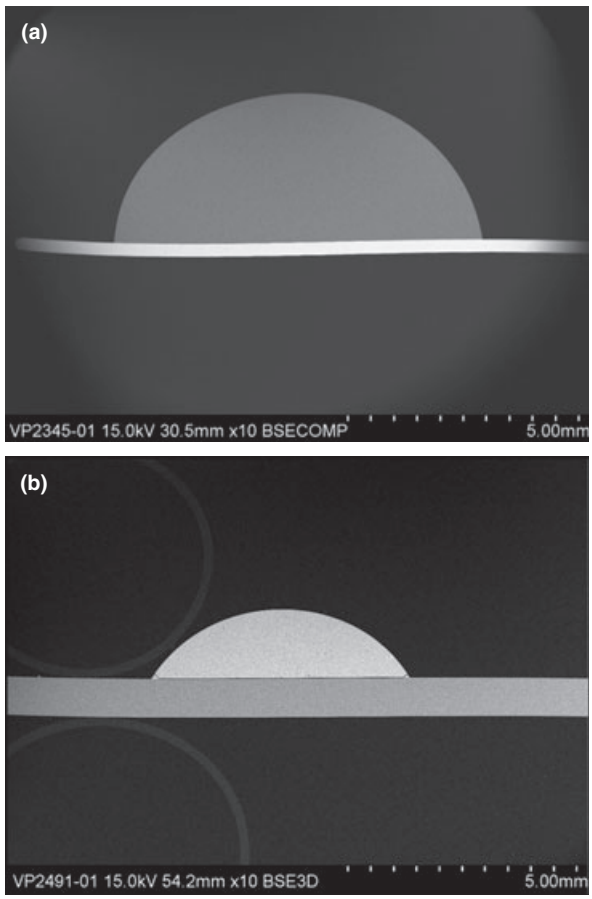


*Fig. 2. Scanning electron micrographs illustrating the microstructure of (a) SCN-1 and G6 (b) glasses in the as-sintered condition. The distortion in the substrate in Figure 2a is an artifact of the SEM when imaging at low magnification.*

Figure 4 shows the thermal expansion behavior of G6, which exhibits behavior comparable to that of SCN-1. The coefficient of thermal expansion of G6 also exhibits a slight temperature dependency between 25 and 500°C, which can be expressed as:

$$\alpha(T) = 7.25 \times 10^{-6} + (6.67 \times 10^{-9})T \quad (^{\circ}C^{-1}) \quad (2)$$

where $T$ is in degrees Celsius.

The glass transition temperature is a key parameter because it determines the transition point where the

**Table I. Chemical Composition of SCN-1 Glass; G6 Glass**

| | Weight% | |
|---|---|---|
| **Element** | **ICP-MS** | **ICP-AES** |
| SCN−1 | | |
| Si | 51.9 | 54.8 |
| K | 15.0 | 13.4 |
| Ba | 14.0 | 12.9 |
| Na | 9.8 | 8.3 |
| Ca | 3.9 | 5.0 |
| Al | 3.4 | 3.4 |
| Mg | 1.2 | 1.3 |
| Ti | 0.5 | 0.6 |
| B | 0.1 | 0.1 |
| Zn | 0.1 | 0.0 |
| G6 | | |
| Si | 50.5 | 53.4 |
| Na | 15.5 | 12.6 |
| Ba | 7.7 | 7.2 |
| B | 6.3 | 6.0 |
| Zn | 5.8 | 5.8 |
| Al | 5.2 | 5.1 |
| Ca | 4.1 | 5.0 |
| K | 3.2 | 3.2 |
| Mg | 1.5 | 1.6 |
| Fe | 0.2 | 0.1 |

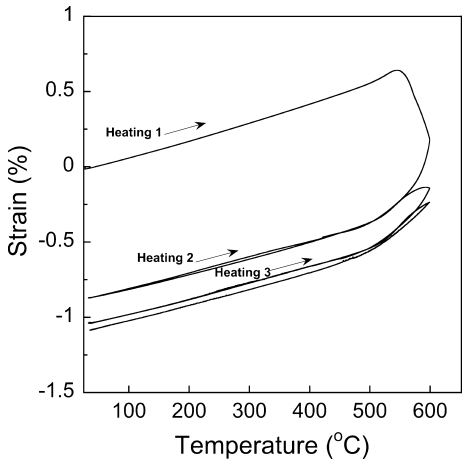


*Fig. 3. Thermal expansion behavior determined at a heating/cooling rate of 5°C/min for SCN-1. Three runs were performed sequentially using a thermomechanical analyzer under different (increasingly smaller) compressive loads (0.10, 0.05, 0.01 N).*

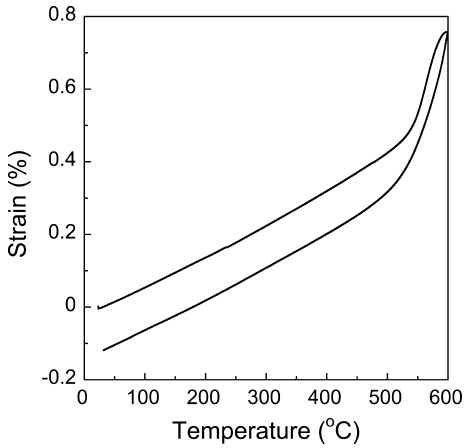


*Fig. 4. Thermal expansion behavior of G6 obtained with a thermomechanical analyzer at a heating/cooling rate of 5°C/min and a constant compressive load of 0.01 N.*

viscosity is sufficiently low to enable glass flow. Values of glass transition temperature of SCN-1 and G6 glasses were determined from the thermal expansion curves according to ASTM E1545.[10] For SCN-1, the glass transition temperature was found to be 468 ± 3° C, and it was found to be insensitive to the magnitude of compressive load. The glass transition temperature of G6 was found to be 508 ± 4°C.

### *Viscosity*

The viscosity of SCN-1 and G6 glasses was determined by the parallel plate technique following standardized test method ASTM C1351.[11] To determine the accuracy of viscosity measurements according to this method using a thermomechanical analyzer, test specimens of standard reference material NIST glass 717a were also evaluated.

For both procedures, changes in the length of the test specimen were used to calculate the viscosity according to the following relationship:

$$\eta = \frac{2\pi\, load\, g\, h^5}{30\, vol \left(\frac{dh}{dt}\right)(2\pi h^5 + vol)} \qquad (3)$$

where $\eta$ is the viscosity (Pas), *load* is the applied load (grams), $g$ is the acceleration due to gravity (cm/s$^2$), *vol* is the volume of the test specimen (cm$^3$), $h$ is the specimen height at time $t$ (cm), and $dh/dt$ is the compression rate (cm/s).[11]

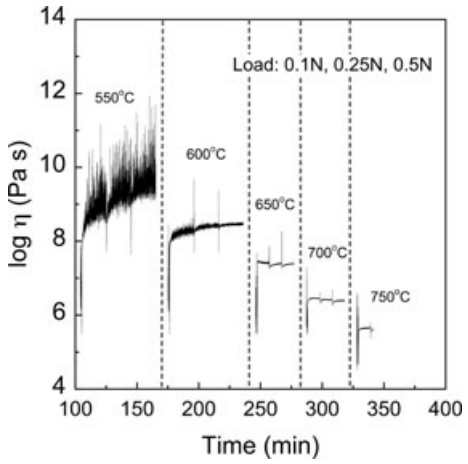


*Fig. 5. Viscosity as a function of time during isothermal tests for SCN-1 glass. At each temperature, three sequential tests were performed at increasingly larger compressive loads.*

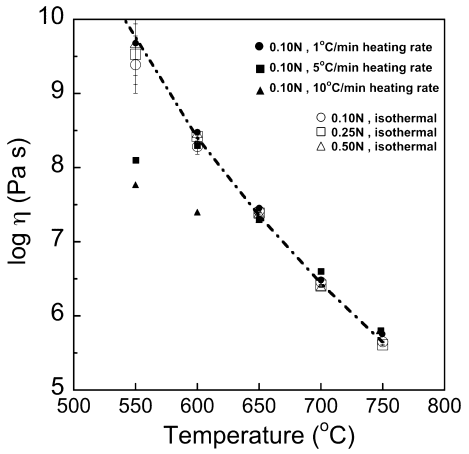


*Fig. 6. Viscosity values of SCN-1 glass obtained under isothermal conditions and under different heating rates. The isothermal tests were performed under different constant compressive loads. Tests under constant heating rate were performed under the same constant load. The error bars represent one standard deviation of the isothermal measurements. The dash line represents the Vogel-Fulcher-Tammann fit of the 0.25 N isothermal data.*

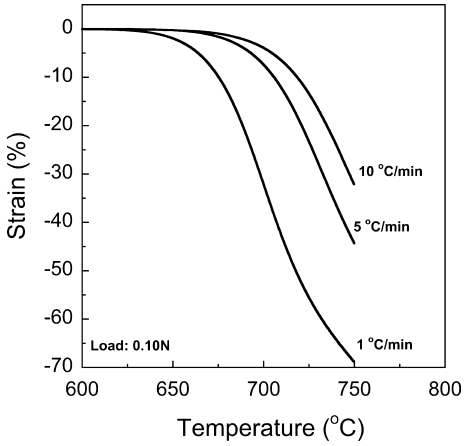


*Fig. 7. Values of displacement recorded as a function of temperature for tests carried out at different heating rates. All tests were performed under a constant compressive load of 0.10 N. The initial test specimen dimensions were 7.3 mm in diameter and 5.5 mm in length.*

It was found using both isothermal and constant heating rate measurements that the viscosity calculated using Eq. (3) is in good agreement with the data provided in the certificate of the standard reference material. The error was found to be 4.4% when comparing viscosity values determined at 700°C under a constant load of 25 g (0.24 N) with reference values.

Viscosity values for SCN-1 glass were obtained under isothermal conditions with varying dwell time. At lower temperatures, it took a longer period of time for the viscosity to reach an equilibrium value. Also, noise was greatest at the lowest temperature as illustrated by the results in Fig. 5.

The viscosity of SCN-1 was found to be independent of the applied load at any temperature, suggesting that the glass behaves as a Newtonian fluid for the range of conditions used in these experiments. The temperature dependence of the viscosity could be described by the Vogel-Fulcher-Tammann (VFT) model, according to the following equation:

$$\log_{10}[\eta] = -6.007 + \frac{9129.7}{T + 33.46} \qquad (4)$$

where $T$ is temperature in degrees Centigrade. The fitted function is presented in Fig. 6 (dashed line) along with the results from isothermal tests.

The viscosity of the glass was also determined by recording the change in the test specimen length while heating under a constant heating rate and constant compressive load. Figure 7 shows the deformation of a test specimen recorded using a thermomechanical analyzer at temperatures between 600 and 750°C. The curves in Fig. 7 correspond to tests performed at heating rates of 1, 5 and 10°C/min and a constant load of

0.1 N. From these curves, the viscosity of the glass was determined using Eq. (3). The results are also included in Fig. 6 along with results obtained from isothermal tests. At temperatures below 600°C, the calculated values of viscosity at heating rates of 5 and 10°C/min are lower than those determined from isothermal tests. At temperatures above 600°C, results obtained by both the isothermal and constant heating rate methods are in good agreement. The discrepancy of results at temperatures below 600°C is most likely the result of differences in the actual temperature of the glass and that recorded by the thermocouple used to control the operation of the furnace. The same methodology was used to determine the viscosity of G6 glass, and the temperature dependence of its viscosity could be described with a Vogel-Fulcher-Tammann (VFT) fit according to the following equation:

$$\log_{10}[\eta] = -3.126 + \frac{3917.5}{T - 295.45} \qquad (5)$$

where $T$ is temperature in degrees Centigrades.

### *Elastic Constants*

The determination of elastic constants by resonant ultrasound spectroscopy requires knowing the density of the material. Therefore, the values of thermal expansion obtained for both SCN-1 and G6 glasses were used to determine their density as a function of temperature.

The Young's modulus values of SCN-1 and G6 glasses as a function of temperature are plotted in Fig. 8. The Young's modulus of SCN-1 was found to decrease from 51.9 GPa at room temperature to 49.8 GPa at 400°C while its Poisson's ratio remained nearly constant at 0.22. Data were collected during cooling and the values obtained during heating and cooling were found to be equivalent. Error bars are also included in the plot, although they are small and difficult to discern. Attempts to determine values of the elastic constants of SCN-1 above 400°C were unsuccessful because of the broadening of the spectra peaks. The Young's modulus of G6 was found to decrease linearly with temperature from 72.8 GPa at 25°C to 68.5 GPa at 500°C at a rate of $9.05 \times 10^{-3}$ GPa/°C, while its Poisson's ratio remained constant with a value of 0.23. At higher temperatures, the Young's modulus of G6 decreased linearly with temperature but at a rate

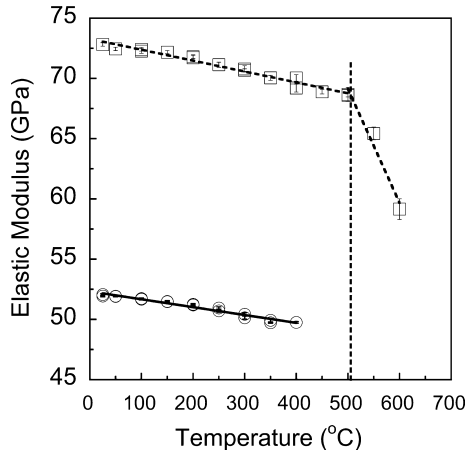


*Fig. 8. Young's modulus as a function of temperature for SCN-1 and G6 determined by resonant ultrasound spectroscopy. Squares correspond to G6. Circles to SCN-1. The error bars represent the root mean square error of the fit. The vertical line indicates the glass transition temperature.*

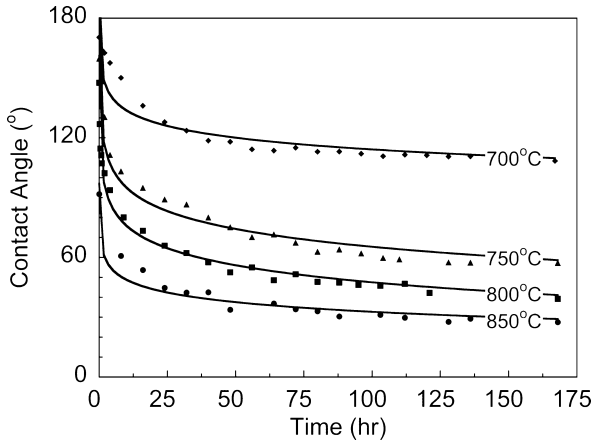


*Fig. 9. Contact angle between SCN-1 and 8YSZ substrates as a function of temperature and time. The time dependence of the contact angle arises from gravitational effects.*

10 times greater ($9.45 \times 10^{-2}$ GPa/°C) to a value of 59.2 GPa at 600°C.

### *Wetting*

Figure 9 shows values of the contact angle between SCN-1 and 8YSZ between 700 and 850°C as a function of time. For any given time, the dynamic contact angle decreases with increasing temperature. At the start

of the test, the contact angle decreased rapidly and for longer times, it continued to decrease in value but at a lower rate. After 168 h, the contact angle at 850°C was <30°. It was found that the contact angle between G6 and 8YSZ was lower than that between SCN-1 and 8YSZ for times less than 40 h and the values exhibited a weaker time dependency.

## Discussion

Crystallization-resistant glasses are being considered for SOFC sealing applications.[2–5] These materials are attractive because of their self-healing characteristics, their ability to relax thermal stresses *via* viscous flow at SOFC operating temperatures and because properties like their viscosity, glass transition temperature, thermal expansion and elastic modulus can be tailored by changing their composition.

In this study, we have presented values for several physical and mechanical properties of SCN-1 and G6 glasses, which are relevant for assessing their feasibility as SOFC seals. These data are also useful for models of the thermomechanical behavior of SOFCs that incorporate these glasses in their design.

One of the most important parameters in glass sealing applications is thermal expansion behavior. It is critically important to ensure that the thermal expansion of the glasses at temperatures below their glass transition temperature is compatible with those of the materials with which it will be in contact in the stack. In the case of planar SOFCs, these include the electrolyte and interconnects. While the thermal expansion of the glasses exhibits slight temperature dependence up to the glass transition temperature, their values are in the range of thermal expansion values reported for barium silicate glasses[2,12] and comparable to values reported for alkali-alkaline-earth silicates.[13]

These values are also comparable to the coefficient of thermal expansion of 8YSZ, which increases slightly with temperature from $8.5 \times 10^{-6}$/°C at 100°C to $10.5 \times 10^{-6}$/°C at 950°C[14] and that of ferritic stainless steels, which are being considered for metallic interconnects for planar SOFCs. For example, the linear coefficients of thermal expansion between 20 and 500°C are $11.5 \times 10^{-6}$/°C for alloy 441[15] and $11.2 \times 10^{-6}$/°C for Crofer 22 APU.[16] Matching the thermal expansion of glass seals to those of interconnects, and the electrolyte is important to minimize residual stresses in the stack during cooling at temperatures below the glass transition temperature of the glass seal.

The glass transition temperature is also a key parameter to decide whether or not a crystallization-resistant glass can be used for SOFC sealing applications. The glass transition temperature has to be lower than the operating temperature of the SOFC to ensure the glass can flow and function as a sealant. Similarly, the softening temperature of glasses for sealing applications must be sufficiently high, or the applied compressive load must be sufficiently low, to prevent squeezing the glass from the stack. The results in Fig. 3 illustrate this behavior as the lateral viscous flow of these glasses increases with the magnitude of the applied compressive load. If the softening temperature is not sufficiently high, seals containing viscous glasses need to be engineered to prevent this from happening. These seals can be engineered, for example, by using rigid dimensional separators[5] or by adding rigid second phases that are thermochemically compatible with the glass.

At the glass transition temperature of both SCN-1 and G6, there is a significant increase in the rate of thermal expansion with temperature. However, this change is accompanied with a significant decrease in stiffness (Fig. 8), which results in the relaxation of any stresses that might have resulted from mismatches in thermal expansion with the neighboring components. The value obtained for the glass transition temperature of G6 according to standard test method ASTM E1545 (508°C) was found to be consistent with the temperature (505°C) at which the rate of decrease of Young's modulus with temperature increased by a factor of 10 (Fig. 8).

Values of the elastic properties of glasses are essential to predict residual stresses in the stack during cooling below the glass transition temperature of glass seal. Changes in elastic properties can also be used as a means to monitor microstructural changes in the glass (e.g., from the precipitation of crystalline phases or evolution of pore size distribution). While there are no specific targets for the magnitude of the elastic modulus of crystallization-resistant glasses for sealing SOFCs, it is worth considering that the magnitude of stresses in these glasses, which arise from mismatches in thermal expansion with surrounding SOFC components is proportional to the difference in coefficients of thermal expansion and to the magnitude of Young's modulus for the glass. Therefore, more compliant glasses would be preferred for this application.

Makishima and Mackenzie derived an equation to estimate the Young's modulus of oxide glasses from their chemical composition.[17] Their method is based on a consideration of the dissociation energy of the oxide constituents and their packing density.

$$E = 2V_T \sum_i X_i G_i \tag{6}$$

$$V_T = \frac{\rho}{M} \sum_i V_i X_i \tag{7}$$

where E is the Young's modulus of the glass, $M$ is the effective molecular weight, ρ is the density, $X_i$ is the mole fraction of component $i$, and $V_i$ and $G_i$ are its packing factor and dissociation energy per unit volume. Values of $V_i$ and $G_i$ are listed in reference 17 for several oxides. Using the ICP-AES compositional information listed in table I for SCN-1 and G6, the Young's modulus of SCN-1 and G6 were predicted to be 70.2 and 71.8 GPa, respectively. ICPAES values were selected for this calculation because they have smaller uncertainty associated. While the value predicted for G6 is within 1.3% of the value determined by resonant ultrasound spectroscopy, there is a large discrepancy between the value predicted for SCN-1 and that determined experimentally. However, by accounting for the 18% porosity in SCN-1 and using the rule of mixtures, the predicted Young's modulus of SCN-1 is 57 GPa, which is within 9% of the value determined experimentally by resonant ultrasound spectroscopy. Porosity not only affects the physical and mechanical properties of glasses, but it is undesirable for sealing applications.

Accurate methods for chemical compositional analysis are needed to estimate key properties, as exemplified by the use of the Makishima-Mackenzie model to predict Young's modulus. In this study, chemical compositional values obtained by ICP-MS and ICP-AES were found to be consistent with those supplied by the glass manufacturers. Accurate compositional analyses are also needed to assess the long-term stability of glasses in SOFC environments. A recent study conducted by the authors was focused on determining how the chemical composition of glasses change when these were exposed to air or gas mixtures of $H_2$+$N_2$+$H_2O$ at 800°C, as a function of time, for periods of time in excess of 10,000 h.[18] Such changes in the glass chemical composition might result, for example, from evaporation of certain elements or from the precipitation of crystalline phases. These studies have revealed that crystalline phases of barium oxide, cristobalite, $MgCaSi_2O_6$, $CaSiO_3$ and $KAlSi_3O_8$ precipitate as a function of time, with corresponding changes in the composition of the glass. However, based on the estimates of the rates of crystallization and growth of these phases and the initial concentration in the glass of elements present in these crystalline phases, it is predicted that the volume fraction of these phases (e.g., $KAlSi_3O_8$) would not exceed concentrations greater than 16 vol.% after 40,000 h.[18] Furthermore, the glass transition temperature of these glasses was found to remain constant for at least 12,000 h exposure in air or gas mixtures of $H_2$+$H_2O$+$N_2$.

The Vogel-Fulcher-Tammann model was found to provide an accurate representation of the temperature dependence of the viscosity of both glasses, while the time-dependence of viscosity of SCN-1 at lower temperatures can be attributed to structural relaxation of the glass. The discrepancy of results at temperatures below 600°C is most likely the result of differences in the actual temperature of the glass and that recorded by the thermocouple used to control the operation of the furnace.

The gradual increase in viscosity with time is an indication that the sample has a fictive temperature higher than the thermocouple temperature used to control the operation of the furnace.[7] At higher temperatures, the difference between the fictive temperature and that used to control the operation of the furnace decreases. Overall, the viscosity of SCN-1 and G6 glasses is in the range of $4 \times 10^5$–$3 \times 10^9$ Pa-s, which is deemed appropriate for SOFC applications.[1,4]

The contact angle between SCN-1 and G6 and both 8YSZ and $Al_2O_3$ substrates was found to decrease with time. Under dynamic wetting conditions, the rate at which a liquid drop spreads on a surface is influenced by temperature, the characteristics of the surface (e.g., texture), the volume of the drop, the characteristics of the liquid (e.g., viscosity) and the characteristics of the liquid–surrounding environment interface.[19] As the volume of the drop decreases, gravitational effects become less and less important. Given the dimensions of the test specimens used to determine contact angle in this study, it is clear that gravitational forces and viscous flow are the main mechanisms responsible for the time dependency of

the contact angle values. The dimensions of the test specimens used in this investigation were selected to facilitate the handling of test specimens and their analysis. However, these dimensions are much greater than those of seals in SOFCs and therefore, the time-dependence of wetting behavior in actual SOFC glass seals is expected to be insignificant.

## Summary

The physical and mechanical properties of SCN-1 and G6 glasses were determined in air as a function of temperature. Viscosity was determined between 550 and 750°C by two different techniques. Both glasses were found to be Newtonian and values obtained by the two techniques are in good agreement except at temperatures below 600°C. The temperature dependence of their viscosity can be described using the Vogel-Fulcher-Tammann model. The Young's modulus and Poisson's ratio of both glasses were determined by resonant ultrasound spectroscopy up to 550°C. The elastic modulus of SCN-1 exhibited a slight linear temperature dependence up to 400°C. Similarly, the Young's modulus of G6 decreased linearly with temperature between 25°C and 510°C. For G6 glass, the temperature dependence of the modulus above this temperature and up to 600°C increased tenfold. This transition temperature was found to be close to the value of the glass transition temperature determined from the thermal expansion curves using a thermomechanical analyzer. Values of Young's modulus predicted by the Makishima-Mackenzie model were in excellent agreement with those determined experimentally by resonant ultrasound spectroscopy, particularly after accounting for porosity. The thermal expansion behavior was determined with a thermomechanical analyzer, and it was found to be in the desired range for an SOFC having an 8YSZ electrolyte and ferritic stainless steel interconnects. Both glasses were found to wet both 8YSZ and $Al_2O_3$ substrates, and overall, their properties were found to be adequate for use as crystallization-resistant seals for SOFCs.

The electrical properties of glasses that would be used for SOFC sealing applications are as important as their mechanical properties. This is particularly true for glasses like SCN-1 and G6, which contain alkaline earth metals. Specifically, glasses for SOFC sealing applications have to be electrically insulating with an electrical resistivity greater than $1 \times 10^4$ Ωm to avoid electrical short circuits.[20] Measurements of the electrical resistivity of SCN-1 and G6 are being performed and will be reported in a future publication.

## Acknowledgments

The authors are grateful for the support of DOE-NETL program managers Rin Burke, Wayne Surdoval, Travis Shultz and Briggs White. The authors are indebted to Mr. Randy Parten and John J. Henry of ORNL for their support preparing test specimens and to Fei Ren and Jane Howe for reviewing the manuscript. Valerie Garcia-Negron was an intern student at Oak Ridge National Laboratory during the preparation of this manuscript. Discussions and collaboration with Y-S Chou and Jeff Stevenson of Pacific Northwest National Laboratory are greatly appreciated. This research work was sponsored by the US Department of Energy, Office of Fossil Energy, SECA Core Technology Program at ORNL.

## References

1. EG&G Technical Services (Ed)., *Fuel Cell Handbook*, 7th edition, U.S. Department of Energy, Office of Fossil Energy, Morgantown, WV, 2004.
2. J. W. Fergus, "Sealants for Solid Oxide Fuel Cells," *J. Power Sources*, 147 46–57 (2005).
3. R. N. Singh, "Sealing Technology for Solid Oxide Fuel Cells (SOFC)," *Int. J. Appl. Ceram. Technol.*, 4 [2] 134–144 (2007).
4. M. K. Mahapatra and K. Lu, "Glass-Based Seals for Solid Oxide Fuel and Electrolyzer Cells – A Review," *Mater. Sci. Eng., R*, 67 65–85 (2010).
5. Y.-S. Chou, *et al.*, "Compliant Alkali Silicate Sealing Glass for Solid Oxide Fuel Cell Applications: Thermal Cycle Stability and Chemical Compatibility," *J. Power Sources*, 196 2709–2716 (2011).
6. J. M. Giaquinto, C. K. Bayne, D. C. Glasgow, R. H. Ilgner, and T. J. Keever, "Uncertainty Study for the Measurement of Elemental Composition in Glass Specimens," Oak Ridge National Laboratory Internal Report (2010).
7. J. Wang, "Glass Viscosity Rheometry and Structural Relaxation by Parallel Plate Using a Thermo-Mechanical Analyzer," *Mater. Lett.*, 31 99–103 (1997).
8. A. Migliori and J. L. Sarrao, *Resonant Ultrasound Spectroscopy*, Wiley-Interscience, New York, NY, 1997.
9. M. Radovic, E. Lara-Curzio, and L. Riester, "Comparison of Different Experimental Techniques for Determination of Elastic Properties of Solids," *Mater. Sci. Eng.*, A368 56–70M (2004).
10. ASTM-E1545, Standard Test Method for Assignment of the Glass Transition Temperature by Thermomechanical Analysis.
11. ASTM-C1351, Measurement of Viscosity of Glass Between $10^4$ Pa·s and $10^8$ Pa·s by Viscous Compression of a Solid Right Cylinder.
12. P. Geasee, T. Schwickert, U. Diekmann, and R. Conradt, "Glasses from the System $RO\text{-}R_2O_3\text{-}SiO_2$ As Sealants of High Chromium Steel Compo-

nents in the Planar SOFC," *Ceramic Materials and Components for Engines*, eds., J. G. Heinrich and F. Aldinger. Wiley-VCH Verlag GmbH, Weinheim, Germany, 57–62, 2001.
13. T. Rouxel, "Elastic Properties and Short-to Medium-Range Order in Glasses," *J. Am. Ceram. Soc.*, 90 [10] 3019–3039 (2007).
14. E. Radovic, R. Lara-Curzio, H. Trejo, H. Wang, and W. D. Porter, "Thermo-Physical Properties of Ni-YSZ as a Function of Temperature and Porosity," *Ceram. Eng. Sci. Proc.*, 27 [4] 79–85 (2006).
15. Allegheny Ludlum, Technical Data, Stainless Steel 441HPTM Alloy.
16. Crofer® 22 APU, Material Data Sheet No. 4046, May 2010 Edition.
17. A. Makishima and J. D. Mackenzie, "Direct Calculation of Young's Modulus of Glass," *J. Non-Cryst. Solids*, 12 35–45 (1973).
18. E. Lara-Curzio, *et al.* Unpublished results.
19. L. Leger and J. F. Joanny, "Liquid Spreading," *Rep. Prog. Phys.*, 55 431–486 (1992).
20. C. Lara, M. J. Pascual, R. Keding, and A. Duran, "Electrical Behaviour of Glass–Ceramics in the Systems RO–BaO–$SiO_2$ (R = Mg, Zn) for Sealing SOFCs," *J. Power Sources*, 157 377–384 (2006).